

**Angular Momentum Transfer via Relativistic Spin-Lattice Coupling from First Principles**Sergiy Mankovsky<sup>1</sup>, Svitlana Polesya<sup>1</sup>, Hannah Lange<sup>1</sup>, Markus Weißenhofer<sup>2</sup>,  
Ulrich Nowak<sup>2</sup> and Hubert Ebert<sup>1</sup><sup>1</sup>*Department of Chemistry/Physical Chemistry, LMU Munich,  
Butenandtstrasse 11, D-81377 Munich, Germany*<sup>2</sup>*Department of Physics, University of Konstanz, DE-78457 Konstanz, Germany*

(Received 30 March 2022; accepted 15 July 2022; published 5 August 2022)

The transfer and control of angular momentum is a key aspect for spintronic applications. Only recently, it was shown that it is possible to transfer angular momentum from the spin system to the lattice on ultrashort timescales. To contribute to the understanding of angular momentum transfer between spin and lattice degrees of freedom we present a scheme to calculate fully relativistic spin-lattice coupling parameters from first principles. In addition to the dipole-dipole interactions often discussed in the literature, these parameters give, in particular, access to the spin-lattice effects controlled by spin-orbit coupling. By treating changes in the spin configuration and atomic positions at the same level, closed expressions for the atomic spin-lattice coupling parameters can be derived in a coherent manner up to any order. Analyzing the properties of these parameters, in particular their dependence on spin-orbit coupling, we find that even in bcc Fe the leading term for the angular momentum exchange between the spin system and the lattice is a Dzyaloshinskii-Moriya-type interaction, which is due to the symmetry breaking distortion of the lattice.

DOI: [10.1103/PhysRevLett.129.067202](https://doi.org/10.1103/PhysRevLett.129.067202)

Spintronics is an emerging field aiming for the development of future nanoelectronic devices. A key aspect is the transport and control of angular momentum [1]. While the focus has long been on spin-polarized electrons to carry the angular momentum, newer lines of research include the magnonic spin as angular momentum carrier, opening perspectives for insulator spintronics. Understanding the flow of angular momentum is also vital for the progress of ultrafast magnetization switching. In certain ferrimagnets, a single laser pulse can switch the magnetization orientation on a subpicosecond timescale [2], due to the exchange of spin angular momentum between the two magnetic sublattices [3,4]. However, recent work on ultrafast demagnetization in ferromagnets has demonstrated that angular momentum can also be transferred from the spin system to the lattice on similar time scales [5]. In the lattice, the spin angular momentum is absorbed in terms of phonons carrying the angular momentum until—on larger timescales—the macroscopic Einstein–de Haas effect sets in [6]. These findings add another piece to the mysteries of spintronics and ultrafast phenomena, namely, the understanding of the microscopic mechanisms that transfer angular momentum between the spin system and the lattice.

The calculation of spin-lattice coupling (SLC) terms, including the exchange of angular momentum between spins and lattice degrees of freedom, is only at its beginning [7–10]. The development of new tools for the quantitative calculation of spin lattice dynamics—so-called molecular-spin dynamics simulations [11–15]—is delayed by the fact

that a systematic derivation of proper spin-lattice parameters is still missing. For a pure spin model the calculation of exchange coupling parameters  $J_{ij}$  of the Heisenberg Hamiltonian by means of the so-called Lichtenstein formula [16] is a well-established approach to supply the input for Monte Carlo [17] as well as spin-dynamics simulations [18,19]. Corresponding extensions of this computational scheme are available to account for the full tensorial form of the interaction parameters [20,21] as well as their extension to a multispin formulation [22].

Including the lattice degrees of freedom is much more challenging. A practical scheme to calculate microscopic SLC parameters quantitatively and on the basis of electronic structure calculations has been suggested so far only by Hellsvik *et al.* [14] by applying the Lichtenstein formula as well as its relativistic generalization [23] for a system with one atom moved gradually from its equilibrium position.

In this Letter we present and exploit an improved, fully relativistic scheme that treats changes to the spin configuration and atomic positions on the same level. This allows us to derive closed expressions for the atomic SLC parameters in a coherent way up to any order. First numerical results are presented for the three-site terms of bcc Fe. Surprisingly, even in a bcc crystal the leading term for the exchange of spin angular momentum with the lattice is a Dzyaloshinskii-Moriya-type interaction emerging due to the symmetry breaking distortion of the lattice.

To describe the coupling of spin and spatial degrees of freedom we adopt an atomistic approach and start

with the expansion of a phenomenological spin-lattice Hamiltonian

$$\begin{aligned} \mathcal{H}_{sl} = & - \sum_{i,j,\alpha,\beta} J_{ij}^{\alpha\beta} e_i^\alpha e_j^\beta - \sum_{i,j,\alpha,\beta} \sum_{k,\mu} \mathcal{J}_{ij,k}^{\alpha\beta,\mu} e_i^\alpha e_j^\beta u_k^\mu \\ & - \sum_{i,j} \sum_{k,l} \mathcal{J}_{ij,kl}^{\alpha\beta,\mu\nu} e_i^\alpha e_j^\beta u_k^\mu u_l^\nu, \end{aligned} \quad (1)$$

that can be seen as a lattice extension of a Heisenberg model. Accordingly, the spin and lattice degrees of freedom are represented by the orientation vectors  $\hat{e}_i$  of the magnetic moments  $\vec{m}_i$  and displacement vectors  $\vec{u}_i$  for each atomic site  $i$ . In Eq. (1) we omit pure lattice terms that involve the force constants [14] as we focus here on the magnetic part of the Hamiltonian. The pure spin part (term 1) has been restricted to its two-site contributions with the corresponding coupling parameters denoted two-site SSC (spin-spin coupling) below. An extension accounting for higher order multispin-lattice interactions can be done in a straightforward manner [22]. Also, the SLC has been restricted to three and four-site terms (terms 2 and 3). As relativistic effects are taken into account, the exchange and spin-lattice interactions are described in tensorial form [20,22], i.e.,  $J_{ij}^{\alpha\beta}$ ,  $\mathcal{J}_{ij,k}^{\alpha\beta,\mu}$ , and  $\mathcal{J}_{ij,kl}^{\alpha\beta,\mu\nu}$ . The Hamiltonian in Eq. (1) is similar in form to the one discussed by Hellsvik *et al.* [14], potentially providing a suitable basis for advanced molecular-spin dynamics simulations.

In previous works expressions for the exchange coupling parameters  $J_{ij}$  [16] or  $J_{ij}^{\alpha\beta}$  [20,21], respectively, have been derived by mapping the free energy landscape  $\mathcal{F}(\{\hat{e}_i\})$  obtained from first-principles electronic structure calculations on the Heisenberg spin Hamiltonian. Here, we follow the same strategy by mapping the free energy landscape  $\mathcal{F}(\{\hat{e}_i\}, \{\vec{u}_i\})$  accounting for its dependence on the spin configuration  $\{\hat{e}_i\}$  as well as atomic displacements  $\{\vec{u}_i\}$  on the same footing. Making use of the magnetic force theorem the change in free energy  $\Delta\mathcal{F}$  induced by changes of the spin configuration  $\{\hat{e}_i\}$  with respect to a suitable reference system and simultaneous finite atomic displacements  $\{\vec{u}_i\}$  can be written in terms of corresponding changes to the single-particle energies,

$$\Delta\mathcal{F} = \int^{E_F} dE (E - E_F) \Delta n(E) = - \int^{E_F} dE \Delta N(E), \quad (2)$$

where  $E_F$  is the Fermi energy and  $\Delta n(E)$  and  $\Delta N(E)$  are corresponding changes to the density of states (DOS)  $n(E)$  and integrated density of states  $N(E)$ , respectively.

$\Delta N(E)$  can be evaluated efficiently [16,20,21] via the so-called Lloyd formula when the underlying electronic structure is described by means of the multiple scattering or Korringa-Kohn-Rostoker (KKR) formalism [24]. Adopting this approach we find

$$\Delta\mathcal{F} = -\frac{1}{\pi} \text{ImTr} \int^{E_F} dE [\ln \underline{\underline{\tau}}(E) - \ln \underline{\underline{\tau}}^0(E)], \quad (3)$$

with the so-called scattering path operator  $\underline{\underline{\tau}}^{(0)}(E)$ , where the double underlinement indicates matrices with respect to site and spin-angular momentum indices [24]. Within the KKR formalism these supermatrices, characterizing the reference  $\underline{\underline{\tau}}^{(0)}(E)$  and perturbed  $\underline{\underline{\tau}}(E)$  systems, respectively, are given by

$$\underline{\underline{\tau}}^{(0)}(E) = [\underline{\underline{m}}^{(0)}(E) - \underline{\underline{G}}(E)]^{-1}, \quad (4)$$

with  $\underline{\underline{G}}(E)$  the structure Green's function and  $\underline{\underline{m}}^{(0)}(E) = [\underline{\underline{t}}^{(0)}(E)]^{-1}$  the inverse of the corresponding site-diagonal scattering matrix that carries all site-specific information depending on  $\{\hat{e}_i\}$  and  $\{\vec{u}_i\}$  [24].

Considering a ferromagnetic reference state ( $\hat{e}_i = \hat{z}$ ) with all atoms in their equilibrium positions ( $\vec{u}_i = 0$ ) the perturbed state is characterized by finite spin tiltings  $\delta\hat{e}_i$  and finite atomic displacements  $\vec{u}_i$ . Writing for site  $i$  the resulting changes in the inverse  $t$  matrix as  $\Delta_\mu^s \underline{\underline{m}}_i = \underline{\underline{m}}_i(\delta\hat{e}_i^\mu) - \underline{\underline{m}}_i^0$  and  $\Delta_\nu^u \underline{\underline{m}}_i = \underline{\underline{m}}_i(u_i^\nu) - \underline{\underline{m}}_i^0$  allows us to replace the integrand in Eq. (3) by

$$\ln \underline{\underline{\tau}} - \ln \underline{\underline{\tau}}^0 = -\ln(1 + \underline{\underline{\tau}}[\Delta_\mu^s \underline{\underline{m}}_i + \Delta_\nu^u \underline{\underline{m}}_i + \dots]), \quad (5)$$

where all site-dependent changes in the spin configuration  $\{\hat{e}_i\}$  and atomic positions  $\{\vec{u}_i\}$  are accounted for in a one-to-one manner by the various terms on the right-hand side. This implies in particular that the matrices  $\Delta_{\mu(\nu)}^{s(u)} \underline{\underline{m}}_i$  in Eq. (5) are site diagonal and have nonzero blocks only for site  $i$ . Because of the use of the magnetic force theorem these blocks may be written in terms of the spin tiltings  $\delta\hat{e}_i^\mu$  and atomic displacements of the atoms  $u_i^\nu$  together with the corresponding auxiliary matrices  $\underline{\underline{T}}_i^\mu$  and  $\underline{\underline{U}}_i^\nu$  [25], respectively, as

$$\Delta_\mu^s \underline{\underline{m}}_i = \delta\hat{e}_i^\mu \underline{\underline{T}}_i^\mu, \quad (6)$$

$$\Delta_\nu^u \underline{\underline{m}}_i = u_i^\nu \underline{\underline{U}}_i^\nu. \quad (7)$$

Inserting these expressions into Eq. (5) and the result in turn into Eq. (3) allows us to calculate the parameters of the spin-lattice Hamiltonian as the derivatives of the free energy with respect to tilting angles and displacements. With this we derived a new scheme to obtain systematically SLC terms up to any order.

In the following we will restrict ourselves to the third-order SLC parameters, which are linear with respect to the displacements (for more details including the fourth-order SLC parameters see the Supplemental Material [25]). One can write the three-site expression as

$$\mathcal{J}_{ij,k}^{\alpha\beta,\mu} = \frac{\partial^3 \mathcal{F}}{\partial e_i^\alpha \partial e_j^\beta \partial u_k^\mu} = \frac{1}{2\pi} \text{ImTr} \int^{E_F} dE \times [T_i^\alpha \tau_{ij} T_j^\beta \tau_{jk} U_k^\mu \tau_{ki} + T_i^\alpha \tau_{ik} U_k^\mu \tau_{kj} T_j^\beta \tau_{ji}] \quad (8)$$

We will call all these terms three-site SLC terms in the following, even if site indices are identical. The prefactor 1/2 occurs to avoid double counting of the identical terms upon summations in Eq. (1) over indices  $i$  and  $j$ .

Below, we present our first results for the SLC parameters for bcc Fe based on a ferromagnetic reference system with its magnetization  $\vec{M}$  in the  $z$  direction. Furthermore, to check the validity of our new approach for the calculation of  $\mathcal{J}_{ij,k}^{\alpha\beta,\mu}$  we performed also conventional supercell calculations for the two-site SSC parameters  $J_{ij}^{\alpha\beta}(u_k^\mu)$  as a function of displacement  $u_k^\mu$  of atom  $k$ . These calculations have been done for a  $2 \times 2 \times 2$  supercell implying a periodic displacement  $u_k^\mu$ . For the comparison, we multiply our SLC parameters  $\mathcal{J}_{ij,k}^{\alpha\beta,\mu}$  with  $u_k^\mu$  and compare with the SSC parameters  $J_{ij}^{\alpha\beta}(u_k^\mu)$  for varying  $u_k^\mu$ , see Fig. 1, and for a further comparison our Supplemental Material [25]. If not otherwise noted, we restrict ourselves to displacements of atom  $k$  along the  $x$  axis,  $\vec{u}_k || \hat{x}$ .

Since we are especially interested in the exchange of angular momentum between the spin and lattice degrees of freedom we focus on the spin-orbit coupling (SOC) driven elements of the three-site SLC tensor  $\mathcal{J}_{ij,k}^{\alpha\beta,\mu}$ , which give rise to magnetocrystalline anisotropies (MCA) and Dzyaloshinskii-Moriya interactions (DMI) [20] induced by a displacement of atom  $k$ . Figure 1 shows, as an example, the nearest-neighbor SLC products  $\mathcal{J}_{ij,i}^{xy,x} \cdot u_i^x$  compared with the two-site SSC interaction parameters for four groups of atoms as sketched in the inset of Fig. 1.

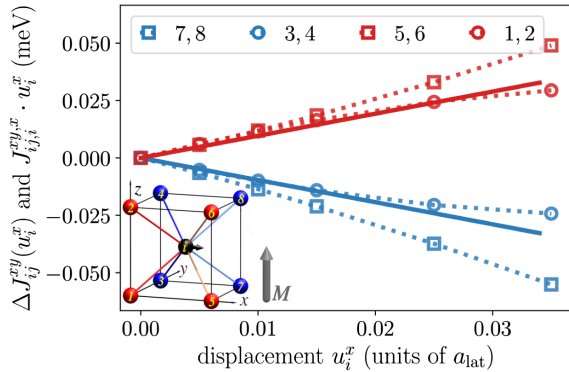


FIG. 1. SLC parameters versus distortion for bcc Fe: Comparison of the products  $\mathcal{J}_{ij,i}^{xy,x} \cdot u_i^x$  (solid lines) with the corresponding SLC terms  $\Delta J_{ij}^{xy}(u_i^x) = J_{ij}^{xy}(u_i^x) - J_{ij}^{xy}(0)$  calculated for a distorted system with the supercell technique (dotted lines) for one atom  $i$  displaced by  $u_i^x$  along the  $x$  axis. The inset shows the labeling of the nearest neighbor atoms used in the figure.

We find good agreement between the different approaches for small amplitudes of the displacement  $u_i^x$ . Please note that the present approach gives direct access to the SLC parameters of any order with respect to the atomic displacement or spin tilting in an extremely efficient way.

The anti-symmetric part of the off-diagonal SLC parameters,  $\mathcal{J}_{ij,k}^{\text{off-a},\mu} = \frac{1}{2}(\mathcal{J}_{ij,k}^{xy,\mu} - \mathcal{J}_{ij,k}^{yx,\mu})$ , can be interpreted [20] as the DMI,  $D_{ij}^z$ , induced by the symmetry-breaking displacement of atom  $k$  and one can define a Dzyaloshinskii-Moriya-like SLC (DSLCL),  $\mathcal{D}_{ij,k}^{z,\mu} = \mathcal{J}_{ij,k}^{\text{off-a},\mu}$ . Note that the conventional DMI vanishes for the non-distorted bcc Fe lattice due to inversion symmetry. Furthermore, for symmetry reasons, all antisymmetric off-diagonal elements of the three-site SLC are equal to zero in the case of a displacement of atom  $k$ , positioned at the same distance from atoms  $i$  and  $j$ , along  $\hat{z}$ , implying  $\mathcal{D}_{ij,k}^{z,z} = 0$ . This does not apply for the other components,  $\mathcal{D}_{ij,k}^{x,z}$  and  $\mathcal{D}_{ij,k}^{y,z}$ .

A further analysis of our SLC parameters is shown in Fig. 2, again for  $i = k$ , which implies that the displacement along the  $x$  direction is applied to one of the interacting atoms. Results for  $k \neq j(i)$  are shown in the Supplemental Material [25]. Different components of the SCL parameters are plotted as a function of the distance  $r_{ij}$ . The absolute values of the DSLCL parameters  $|\vec{D}_{ij,k}^{\mu=x}|$  show a rather slow decay with the distance  $r_{ij}$ . These

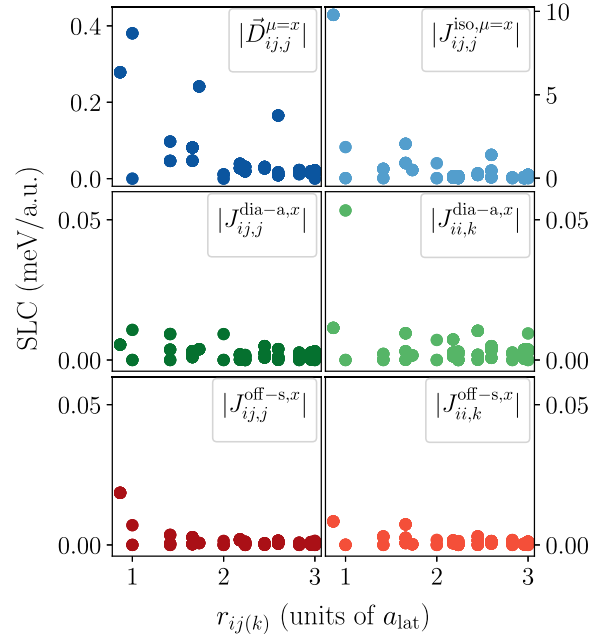


FIG. 2. Magnitude of site-off-diagonal and site-diagonal SLC parameters: DMI  $|\vec{D}_{ij,j}^{\mu=x}|$  and isotropic SLC  $\mathcal{J}_{ij,j}^{\text{iso},\mu=x}$  (top), antisymmetric diagonal components  $\mathcal{J}_{ij,j}^{\text{dia-a},x}$  and  $\mathcal{J}_{ii,k}^{\text{dia-a},x}$  (middle), and symmetric off-diagonal components  $\mathcal{J}_{ij,j}^{\text{off-s},x}$  and  $\mathcal{J}_{ii,k}^{\text{off-s},x}$  (bottom).

parameters can take different values for the same distance, which is a result of the symmetry imposed vanishing of certain components of the DMI-like SLC for some  $\vec{r}_{ij}$  directions, which depend in turn also on the direction of the displacement  $\vec{u}$ . The isotropic SLC parameters  $\mathcal{J}_{ij,j}^{\text{iso},\mu=x} = \frac{1}{2}(\mathcal{J}_{ij,j}^{xx,\mu=x} + \mathcal{J}_{ij,j}^{yy,\mu=x})$ , which have only a weak dependence on the SOC, are about 1 order of magnitude larger than the DSLC. All other SOC-driven parameters shown in Fig. 2, characterizing the displacement-induced contributions to MCA, are much smaller than the DSLC. Note that the DSLC is material specific and can be stronger, e.g., in the case of magnetic overlayers deposited on a heavy-element substrate [25]. A more detailed analysis of the key role of the SOC for three-site SLC parameters is given in the Supplemental Material [25].

So far, we have analyzed the SLC parameters in terms of their impact on the spin-spin interactions for given displacements of the atoms. Additionally, our spin-lattice Hamiltonian, Eq. (1), predicts the inverse phenomenon: a noncollinear spin configuration gives rise to forces acting on the atoms, where the forces can be calculated as  $\vec{F} = -(\partial\mathcal{H}_{\text{sl}}/\partial\vec{u}_k)$  [19]. The emerging forces for an exemplary noncollinear spin configuration, a single spin rotated by  $\pi/2$  in an otherwise collinear configuration, are shown in Fig. 3. These forces are decomposed into their longitudinal and perpendicular parts (with respect to the distance vector  $\vec{r}_{ij}$ ) and whether they come from isotropic, DMI-type or MCA-type contributions to the SLC parameters. The main contribution to the longitudinal forces, which do not transfer angular momentum, comes once again from the isotropic Heisenberg interaction. However, the largest perpendicular—and with that angular momentum transferring—component is once again due to the DMI-type interaction. Plugging in numbers for the mass of an Fe atom we note that the latter is sufficient to accelerate a free Fe atom within 100 fs to a velocity of about 1 m/s.

The role of the DMI-like SLC parameters for the spin-lattice angular momentum transfer can also be discussed in terms of magnon-phonon interactions [7,9,10,37]. With this in mind, we represent the second term of the Hamiltonian in Eq. (1), in terms of isotropic and anisotropic interactions focusing on the DSLC contribution

$$\mathcal{H}_{\text{me-DMI}} = \frac{1}{S^2} \sum_{i,j} \sum_{k,\mu} \vec{D}_{ij,k}^{\mu} \cdot (\hat{s}_i \times \hat{s}_j) u_k^{\mu}. \quad (9)$$

$\mathcal{H}_{\text{me-DMI}}$  is now given in a form using spin operators  $\hat{s}_i^{\alpha}$  instead of spin orientation vectors  $\hat{e}_i^{\alpha}$ , where  $S$  is the maximal value for spin moment per atom. Introducing spin raising and lowering operators  $\hat{s}_i^{\pm} = \hat{s}_i^x \pm i\hat{s}_i^y$  and using in turn the Holstein-Primakoff transformation [25,38], local spin fluctuations can be represented in terms of canonical boson operators,  $\hat{b}_i^{\dagger}$  and  $\hat{b}_i$ . Performing Fourier

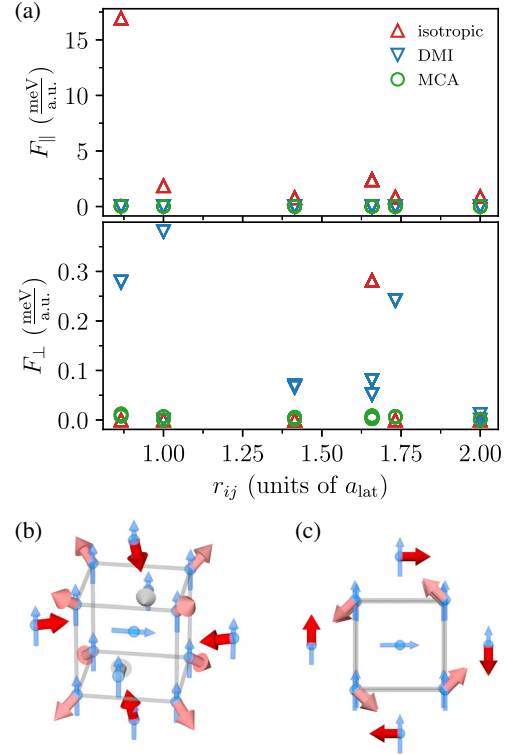


FIG. 3. (a) Longitudinal (top) and perpendicular (bottom) forces (with respect to  $\vec{r}_{ij}$ ) emerging from the isotropic, DMI-type and MCA-type contributions to the SLC parameters. The central spin at  $\vec{r} = (0, 0, 0)$  is tilted in the  $y$  direction while all the others point in the  $z$  direction [blue arrows in (b) and (c)]. (b) Directions of the forces with color coding indicating their perpendicular components with red being high and gray being low. (c) Directions of the perpendicular forces.

transformations for the spin operators and the atomic displacements the Hamiltonian  $\mathcal{H}_{\text{me-DMI}}$  can be reduced to the momentum representation form [25]

$$\begin{aligned} \mathcal{H}_{\text{me-DMI}} = & \frac{2i}{\sqrt{2S}} \sum_{\vec{q},\mu} [\mathcal{D}_{\vec{q}}^{-,\mu} \hat{b}_{\vec{q}} - \mathcal{D}_{-\vec{q}}^{+,\mu} \hat{b}_{-\vec{q}}^{\dagger}] u_{\vec{q}}^{\mu} \\ & - \frac{2i}{\sqrt{N}} \frac{1}{S} \sum_{\vec{k},\vec{k}',\mu} \mathcal{D}_{\vec{k},\vec{k}'}^{z,\mu} \hat{b}_{\vec{k}}^{\dagger} \hat{b}_{\vec{k}'} u_{(\vec{k}-\vec{k}')}^{\mu}, \end{aligned} \quad (10)$$

where  $u_{\vec{q}}^{\mu} = \sum_{\lambda} \epsilon_{\lambda,\vec{q}}^{\mu} X_{\lambda,\vec{q}}$  is the eigenvector corresponding to the phonon mode  $(\lambda, \vec{q})$  with the polarization  $\epsilon_{\lambda,\vec{q}}^{\mu}$  (see Supplemental Material [25]). Following the conclusions in Ref. [10], the first term in Eq. (10), which is determined by the DSLC components  $\mathcal{D}_{ij,k}^{x,\mu}$  and  $\mathcal{D}_{ij,k}^{y,\mu}$ , describes the magnon-phonon scattering that allows for an exchange of angular momentum. On the other hand, the DSLC component  $\mathcal{D}_{ij,k}^{z,\mu}$  (with  $z$  the magnetization direction) contributes to the magnon-number conserving scattering characterized by the energy transfer only (see Ref. [10]).

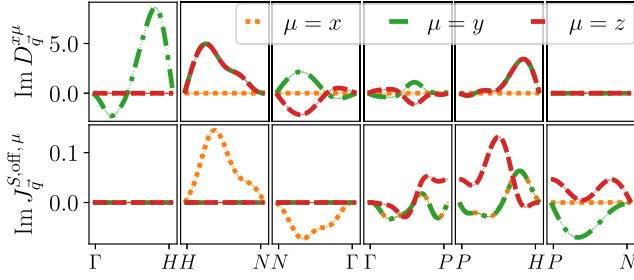


FIG. 4. Imaginary part  $\text{Im}D_{\vec{q}}^{x,\mu}$  (top) and  $\text{Im}(J_{\vec{q}}^{xy,\mu} + J_{\vec{q}}^{yx,\mu})/2$  (bottom) of the SLC parameters for bcc Fe, with  $\mu = x, y, z$ , plotted for  $\vec{q}$  along high-symmetry lines of the Brillouin zone. The real part is zero in all cases.

The upper part of Fig. 4 shows the Fourier transforms  $D_{\vec{q}}^{x,\mu}$  of the SLC parameters for bcc Fe, given by the expression

$$D_{\vec{q}}^{\nu,\mu} = \sum_{j,k} D_{ij,k}^{\nu,\mu} e^{i\vec{q}\cdot(\vec{R}_j - \vec{R}_i)} e^{-i\vec{q}\cdot(\vec{R}_k - \vec{R}_i)}, \quad (11)$$

which are plotted for  $\vec{q}$  along the high-symmetry lines in the Brillouin zone (see also Supplemental Material [25]). One finds for them a strong dependence on the wave vector  $\vec{q}$ . Moreover, this dependence is different for different components of the atomic displacements, which reflects in turn the difference of the magnon-phonon interactions for the transverse and longitudinal phonon modes. However, an efficient angular momentum transfer as well as a strong magnon-phonon coupling, requires the crossing of the phonon and magnon dispersion curves [39,40]. The lower part of Fig. 4 shows the Fourier transforms of the site-diagonal SLC parameters  $\text{Im}(J_{\vec{q}}^{xy,\mu} + J_{\vec{q}}^{yx,\mu})/2$ , with  $\mu = x, y, z$ , which can be seen as a local contribution to the magnetic anisotropy induced by atomic displacements. Comparing the results confirms the dominating role of the DSLC for the magnon-phonon hybridization.

The contribution of the first term in the DSLC Hamiltonian  $\mathcal{H}_{\text{me-DMI}}$  in Eq. (10) to the phonon angular momentum dynamics can also be characterized by the corresponding torque on the phonon spin entering the equation of motion for the phonon angular momentum  $\vec{\mathcal{L}}_{\text{ph}} = \sum_k \vec{u}_k \times \vec{\pi}_k$ , given by  $\vec{T}_{\text{me}} = -\sum_k \vec{u}_k \times (\partial \mathcal{H}_{\text{me}} / \partial \vec{u}_k)$  [10], with the  $\vec{u}_i$  and  $\vec{\pi}_i$  the displacement and linear momentum operators, respectively. The corresponding one magnon-one phonon contribution to the torque,  $\vec{T}_{\text{me}}$  is given by the expression (see Supplemental Material [25])

$$\mathcal{T}_{\text{me-DMI}}^{\gamma} = \frac{2i}{\sqrt{2S}} \sum_{\vec{\lambda}, \vec{q}} [\Gamma_{\vec{\lambda}, \vec{q}}^{-,\gamma} \hat{b}_{\vec{q}} - \Gamma_{\vec{\lambda}, -\vec{q}}^{+,\gamma} \hat{b}_{-\vec{q}}^{\dagger}] X_{\vec{\lambda}, \vec{q}}. \quad (12)$$

Here, the interaction vertices  $\Gamma_{\vec{\lambda}, \vec{q}}^{\pm,\gamma}$  are defined as

$$\Gamma_{\vec{\lambda}, \vec{q}}^{\pm,\gamma} = \epsilon_{\alpha\beta\gamma} [\epsilon_{\vec{\lambda}, \vec{q}}^{\alpha} D_{\vec{q}}^{\pm,\beta} - \epsilon_{\vec{\lambda}, \vec{q}}^{\beta} D_{\vec{q}}^{\pm,\alpha}], \quad (13)$$

with  $\epsilon_{\alpha\beta\gamma}$  the Levi-Civita symbol. As one can see they are fully determined by the DSLC parameters discussed above.

In summary, we present a scheme to calculate microscopic and relativistic SLC parameters from first principles. The perturbation due to a lattice distortion is treated on the same footing as the distortion due to spin tilting, giving access to SLC parameters up to any order for these perturbations. Analyzing the properties of these parameters, in particular their dependence on SOC, we find that even in bcc Fe the leading term that is responsible for the exchange of angular momentum between the spin system and the lattice is a Dzyaloshinskii-Moriya-type interaction, which emerges due to the symmetry breaking distortion of the lattice. Our findings, hence, stress the importance of relativistic effects for the transfer of angular momentum from magnonic excitations to circularly polarized phonons [5,7–10].

Work in Konstanz is supported by the DFG via SFB 1432 and Project No. NO 290/5-1.

- [1] A. Hirohata, K. Yamada, Y. Nakatani, I.-L. Prejbeanu, B. Diény, P. Pirro, and B. Hillebrands, *J. Magn. Magn. Mater.* **509**, 166711 (2020).
- [2] I. Radu, K. Vahaplar, C. Stamm, T. Kachel, N. Pontius, H. A. Dürr, J. Ostler, T. A. Abd Barker, R. F. L. Evans, R. W. Chantrell, A. Tsukamoto, A. Itoh, A. Kirilyuk, T. Rasing, and A. V. Kimel, *Nature (London)* **472**, 205 (2011).
- [3] J. H. Mentink, J. Hellsvik, D. V. Afanasiev, B. A. Ivanov, A. Kirilyuk, A. V. Kimel, O. Eriksson, M. I. Katsnelson, and T. Rasing, *Phys. Rev. Lett.* **108**, 057202 (2012).
- [4] S. Wienholdt, D. Hinzke, K. Carva, P. M. Oppeneer, and U. Nowak, *Phys. Rev. B* **88**, 020406(R) (2013).
- [5] S. R. Tauchert, M. Volkov, D. Ehberger, D. Kazenwadel, M. Evers, H. Lange, A. Donges, A. Book, W. Kreuzpaintner, U. Nowak, and P. Baum, *Nature (London)* **602**, 73 (2022).
- [6] C. Dornes *et al.*, *Nature (London)* **565**, 209 (2019).
- [7] D. A. Garanin and E. M. Chudnovsky, *Phys. Rev. B* **92**, 024421 (2015).
- [8] J. H. Mentink, M. I. Katsnelson, and M. Lemesko, *Phys. Rev. B* **99**, 064428 (2019).
- [9] S. Streib, N. Vidal-Silva, K. Shen, and G. E. W. Bauer, *Phys. Rev. B* **99**, 184442 (2019).
- [10] A. Rückriegel, S. Streib, G. E. W. Bauer, and R. A. Duine, *Phys. Rev. B* **101**, 104402 (2020).
- [11] P.-W. Ma, C. H. Woo, and S. L. Dudarev, *Phys. Rev. B* **78**, 024434 (2008).
- [12] D. Perera, M. Eisenbach, D. M. Nicholson, G. M. Stocks, and D. P. Landau, *Phys. Rev. B* **93**, 060402(R) (2016).
- [13] M. Aßmann and U. Nowak, *J. Magn. Magn. Mater.* **469**, 217 (2019).
- [14] J. Hellsvik, D. Thonig, K. Modin, D. Iuşan, A. Bergman, O. Eriksson, L. Bergqvist, and A. Delin, *Phys. Rev. B* **99**, 104302 (2019).

- [15] M. Strungaru, M. O. A. Ellis, S. Ruta, O. Chubykalo-Fesenko, R. F. L. Evans, and R. W. Chantrell, *Phys. Rev. B* **103**, 024429 (2021).
- [16] A. I. Liechtenstein, M. I. Katsnelson, V. P. Antropov, and V. A. Gubanov, *J. Magn. Magn. Mater.* **67**, 65 (1987).
- [17] S. Polesya, S. Mankovsky, O. Šipr, W. Meindl, C. Strunk, and H. Ebert, *Phys. Rev. B* **82**, 214409 (2010).
- [18] O. N. Mryasov, *Phase Transitions* **78**, 197 (2005).
- [19] B. Skubic, J. Hellsvik, L. Nordström, and O. Eriksson, *J. Phys. Condens. Matter* **20**, 315203 (2008).
- [20] L. Udvardi, L. Szunyogh, K. Palotás, and P. Weinberger, *Phys. Rev. B* **68**, 104436 (2003).
- [21] H. Ebert and S. Mankovsky, *Phys. Rev. B* **79**, 045209 (2009).
- [22] S. Mankovsky, S. Polesya, and H. Ebert, *Phys. Rev. B* **101**, 174401 (2020).
- [23] B. Sadhukhan, A. Bergman, Y. O. Kvashnin, J. Hellsvik, and A. Delin, *Phys. Rev. B* **105**, 104418 (2022).
- [24] H. Ebert, D. Ködderitzsch, and J. Minár, *Rep. Prog. Phys.* **74**, 096501 (2011).
- [25] See Supplemental Material at <http://link.aps.org/supplemental/10.1103/PhysRevLett.129.067202> for additional details on the change of the inverse scattering matrix due to a spin tilting and due to a shift of the atom from the equilibrium position, a comparison of the results on three-site spin-lattice interaction parameters calculated in a relativistic and scalar-relativistic way, as well as the details on the derivation of the magnon-phonon interaction, which includes Refs. [26–36].
- [26] N. Stefanou, P. J. Braspenning, R. Zeller, and P. H. Dederichs, *Phys. Rev. B* **36**, 6372 (1987).
- [27] N. Papanikolaou, R. Zeller, P. H. Dederichs, and N. Stefanou, *Phys. Rev. B* **55**, 4157 (1997).
- [28] S. Mankovsky, S. Polesya, S. Bornemann, J. Minár, F. Hoffmann, C. H. Back, and H. Ebert, *Phys. Rev. B* **84**, 201201(R) (2011).
- [29] H. Böttger, *Principles of the Theory of Lattice Dynamics* (Akademie-Verlag, Berlin, 1983).
- [30] L. Zhang and Q. Niu, *Phys. Rev. Lett.* **112**, 085503 (2014).
- [31] J. P. Elliot and P. G. Dawber, *Symmetry in Physics* (The Macmillan Press Ltd., London, 1979).
- [32] S. Mankovsky, S. Bornemann, J. Minár, S. Polesya, H. Ebert, J. B. Staunton, and A. I. Liechtenstein, *Phys. Rev. B* **80**, 014422 (2009).
- [33] S. Mankovsky, S. Polesya, and H. Ebert, *Phys. Rev. B* **104**, 054418 (2021).
- [34] S.-i. Shamoto, M. Akatsu, M. Matsuura, S. Ohira-Kawamura, K. Harii, M. Ono, L.-J. Chang, T. U. Ito, Y. Nemoto, and J. Ieda, *Phys. Rev. Research* **4**, 013245 (2022).
- [35] H. Ebert *et al.*, The Munich SPR-KKR package, version 8.5, <https://www.ebert.cup.uni-muenchen.de/en/software-en/13-sprkk> (2020).
- [36] S. H. Vosko, L. Wilk, and M. Nusair, *Can. J. Phys.* **58**, 1200 (1980).
- [37] A. Rückriegel, P. Kopietz, D. A. Bozhko, A. A. Serga, and B. Hillebrands, *Phys. Rev. B* **89**, 184413 (2014).
- [38] T. Holstein and H. Primakoff, *Phys. Rev.* **58**, 1098 (1940).
- [39] A. Kamra, H. Keshtgar, P. Yan, and G. E. W. Bauer, *Phys. Rev. B* **91**, 104409 (2015).
- [40] T. Kikkawa, K. Shen, B. Flebus, R. A. Duine, K.-i. Uchida, Z. Qiu, G. E. W. Bauer, and E. Saitoh, *Phys. Rev. Lett.* **117**, 207203 (2016).